Reviewed Preprint
v1 • May 12, 2026
Not revised

For correspondence:
chencwan@gmail.com
xuntu@berkeley.edu
lihuilu1912@gmail.com

* These authors contributed equally

Competing interests: No competing interests declared

Funding: See page 15

Reviewing editor: Karim Fifel, Mohammed VI Polytechnic University, Morocco

Brainwide dopamine dynamics across sleep-wake transitions

Changwan Chen[1,*], Xun Tu[1,*], Lihui Lu[1,*], Cody Pham[1], Xiaofan Zhang[2], Rachel Su[1], Ella Li[1], Zihan Jin[1], Wenqing Cao[1], Yipching Yang[1], Matthew Kihiczak[1], Kristal Hui[1], Dana Darmohray[1]

[1]Department of Neuroscience, Helen Wills Neuroscience Institute, Howard Hughes Medical Institute, University of California, Berkeley, Berkeley, United States • [2]Department of Physiology, Howard Hughes Medical Institute, University of California, San Francisco, San Francisco, United States

eLife Assessment

This study provides **important** insights regarding the temporal dynamics of dopamine across sleep/wake transitions in several brain areas. Using multi-site fiber photometry combined with EEG/EMG recordings, the study revealed heterogenous dynamics across both cortical and several subcortical areas. Although the evidence for these observations is **solid**, evidence for the proposed mechanisms driving DA dynamics is **incomplete**. Overall, the study may have a substantial impact on several fields working on the neurobiology of DA signaling.

https://doi.org/10.7554/eLife.110675.1.sa3

Abstract

Dopaminergic signaling plays a critical role in regulating arousal and transitions between sleep states, yet brainwide dynamics underlying these transitions remain incompletely characterized. Here, we employed multi-site fiber photometry with the dopamine sensor GRAB-DA$_{2m}$, combined with electroencephalogram (EEG)/electromyogram (EMG) recordings, to systematically assess regional dopamine (DA) dynamics across sleep-wake states in the medial prefrontal cortex (mPFC), striatal subregions, central amygdala (CeA), and midbrain nuclei in mice. We found that DA levels prominently increased in the mPFC, dorsolateral striatum (DLS), ventral tegmental area (VTA), substantia nigra pars compacta (SNc), and dorsal raphe nucleus (DRN) during transitions from non-rapid eye movement (NREM) sleep to wakefulness (WAKE), supporting their role in arousal. Conversely, DA decreased in the CeA and nucleus accumbens lateral parts (NAc-L) during these transitions. During transitions from NREM to rapid eye movement sleep (REM), DA elevations were observed in the CeA and middle accumbens subregion (NAc-M), rather than NAc-L, while other regions exhibited decreases. Cross-regional DA correlations revealed synchronized network activity across sleep-wake transitions. Optogenetic activation of VTA and DRN dopamine neurons induced robust DA release in cortical and subcortical regions, and chemogenetic activation promoted wakefulness selectively via VTA and DRN, but not SNc DA neurons. These results elucidate distinct brainwide DA dynamics across state transitions and highlight differential roles for DA signaling in modulating sleep-wake states.

Introduction

Sleep–wake regulation emerges from coordinated activity across distributed neural circuits and neuromodulators systems[1–4]. Among these, dopamine plays a crucial role in arousal, and the gating of behavioral state transitions, with midbrain dopaminergic nuclei projecting broadly to cortical and subcortical targets[5–10]. Dopaminergic neurons in the VTA, SNc, and DRN innervate regions including the mPFC, striatal subregions, and the amygdala, positioning dopamine to influence both global brain states and region-specific computations[11–14].

Prior studies have implicated dopamine in promoting wakefulness and shaping transitions between NREM and REM sleep[1,8,9,15,16]. However, most measurements of dopamine across sleep-wake transition have been constrained to single regions or limited sampling approaches, making it difficult to resolve how dopamine dynamics are coordinated across brainwide during state transitions. Moreover, the heterogeneity of dopaminergic signaling, together with mixed findings regarding its role in sleep regulation, leaves the organization of these signals into functional networks incompletely characterized.

To address these gaps, we asked: How do dopamine levels evolve across sleep–wake transitions in cortical, striatal, amygdalar, and midbrain regions? Are these dynamics synchronized across circuits, and do they reflect functional segregation across WAKE, NREM, and REM sleep? Which dopaminergic populations causally drive these patterns? In this study, we systematically characterized dopamine signaling using multi-site fiber photometry combined with EEG/EMG recordings. We identified brainwide spatiotemporal dynamics of dopamine activity during transitions between sleep and wake states.

Results

Distinct dynamic patterns of dopamine signaling during sleep-wake transitions

To investigate brainwide DA dynamics during different state transitions, we expressed the fluorescent DA sensor GRAB-DA$_{2m}$[17] and implanted optical fibers into 8 brain regions, including the mPFC, NAc-L, NAc-M, DLS, CeA, SNc, VTA, and DRN. Sleep–wake states were classified through simultaneous EEG and EMG recordings (Fig. 1A, B, Fig. S1).

In the mPFC, DA levels increased during transitions from NREM to WAKE and from REM to WAKE (Fig. 1B-D, Fig. S1). Conversely, DA levels decreased during WAKE-to-NREM and NREM-to-REM transitions. In contrast, DA dynamics in the CeA exhibited almost an opposite pattern, with the highest DA levels during REM sleep and the lowest during WAKE (Fig. 1B-D, Fig. S1).

Interestingly, DA dynamics in the striatum displayed distinct temporal patterns across its subregions. In the NAc-M, DA signaling exhibited a transient decrease during NREM-to-WAKE transitions, a robust decrease during REM-to-WAKE transitions, and a marked increase during NREM-to-REM transitions. In the NAc-L, DA levels decreased during NREM-to-WAKE and REM-to-WAKE transitions, increased during WAKE-to-NREM transitions, and exhibited no significant change during NREM-to-REM transitions. Conversely, DA levels in the DLS displayed an opposing trend, with the highest signals during WAKE and the lowest during REM. Notably, DA levels in the DLS also exhibited a transient dip during NREM-to-WAKE transitions (Fig. 1B-D, Fig. S1).

In brain regions containing dopamine neurons, the SNc and VTA shared similar DA dynamics, characterized by a pronounced increase during REM-to-WAKE transitions, a decrease during NREM-to-REM transitions, a slight increase during NREM-to-WAKE transitions, and a decrease during WAKE-to-NREM transitions. In contrast, DA dynamics in the DRN showed partially distinct dynamics, with a robust increase during NREM-to-WAKE transitions, a transient decrease during REM-to-WAKE transitions, and slight decreases during WAKE-to-NREM and NREM-to-REM transitions (Fig. 1B-D, Fig. S1).

Overall, DA levels in the mPFC, DLS, VTA, SNc, and DRN increased during NREM-to-WAKE transitions. During REM-to-WAKE transitions, DA levels in these regions also increased, except for the DRN. These results support the brainwide functional role of DA signaling in wakefulness. DA levels in NAc-L, NAc-M, and CeA decreased during both NREM-to-WAKE and REM-to-WAKE transitions, and increased during NREM-to-REM transitions, which is consistent with previous findings that DA signaling is elevated during NREM and/or REM sleep in these brain areas[15,18].

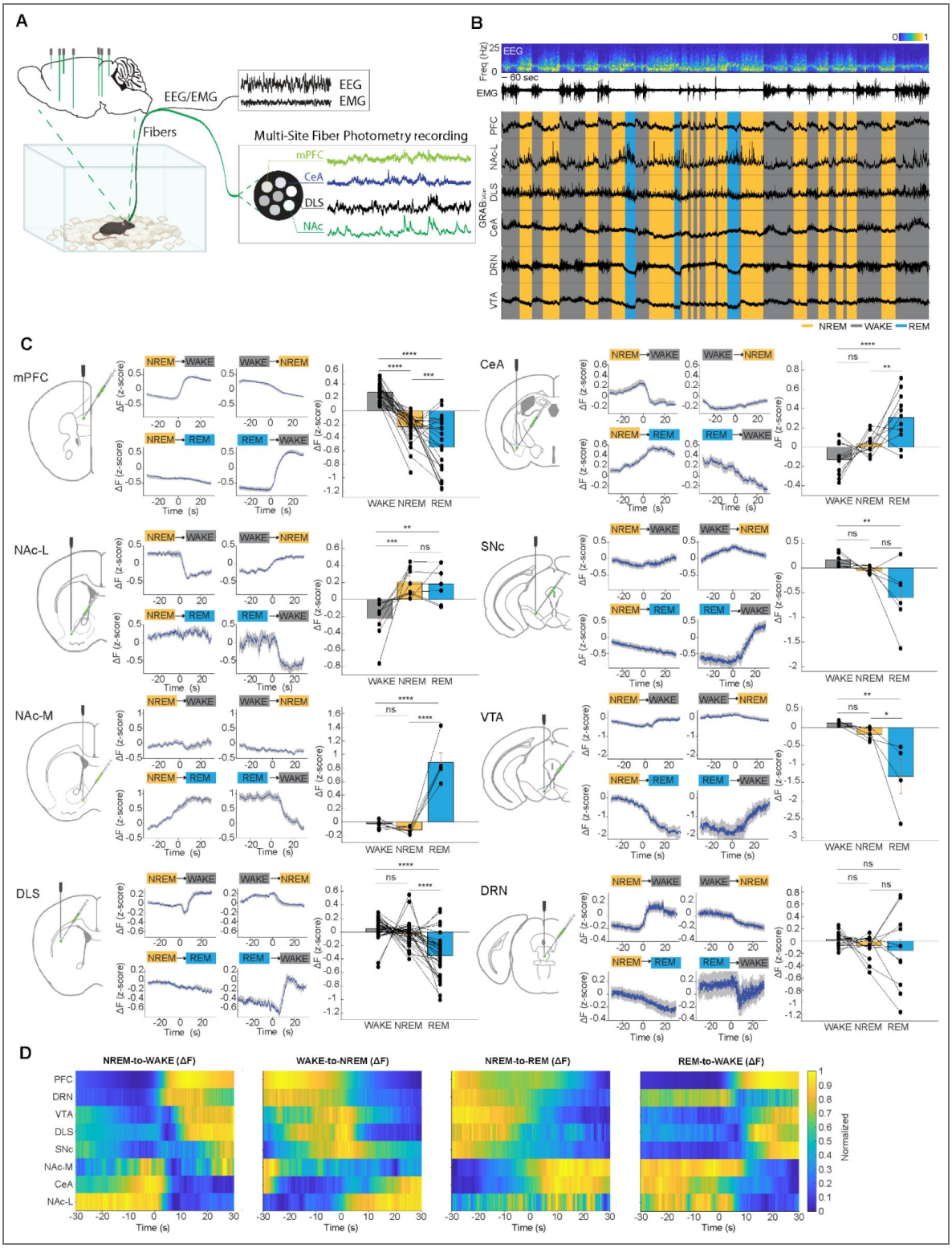

Figure 1. Distinct dynamic patterns of dopamine signaling during sleep-wake states.

(A) Schematic illustration depicting the experimental design in which DA sensor was injected into different downstream targets and EEG/EMG were recorded. **(B)** An example multi-site fiber photometry recording session. Shown are the EEG spectrogram (normalized by the maximum of each session; Freq., frequency), EMG amplitude (Ampl.), brain states (color-coded), and DA signal traces. **(C)** Temporal changes of DA levels in different brain areas at each transition. For each subpanel: Left, schematic of the DA sensor injection and recording site; Middle, DA activity aligned to brain-state transitions (time zero indicates the transition point; shading represents ±s.e.m.); Right, summary of DA activity during WAKE, NREM, and REM, with each dot representing one animal. **(D)** Summary of DA activity (normalized to [0 1]) during 4 brain-state transitions across different brain areas. The data shown here is the average across mice.

DA signaling displays distinct correlation patterns between regions during state transitions

To understand the relationships between different DA signaling during state transitions, we next computed cross-correlations between DA signals in different brain regions and analyzed their temporal dynamics across state transitions. During NREM-to-REM and REM-to-WAKE transitions, DA dynamic changes were generally more synchronized between regions than those during NREM-to-WAKE and WAKE-to-NREM transitions, with less correlation peaks- or troughs-shifting from the time lag t = 0 s (NREM-to-REM: $|t|$ = 1.41 ± 0.48; REM-to-WAKE: $|t|$ = 1.21 ± 0.33; NREM-to-WAKE: $|t|$ = 3.84 ± 0.76; WAKE-to-NREM: $|t|$ = 4.55 ± 1.01. Fig. 2A, 2C, Fig. S2A, 2C).

Across all sleep-wake transition states, DA signaling in the CeA was highly correlated with that in the both NAc-L and NAc-M, as indicated by significant cross-correlation between regions (Fig. 2B, 2D, Fig. S2B, 2D), which also reflected in the temporary correlation dynamics, with high positive values of the correlation peaks at around t = 0 s (Fig. 2A, 2C, Fig. S2A, 2C). Similar correlation dynamics were also observed between PFC and DLS (Fig. 2, Fig. S2). DA signals in these two regions were positively correlated with DA signals in the SNc, VTA, and DRN, respectively, during NREM-to-REM transition and REM-to-WAKE transition. However, DA signals in the NAc-M and CeA are negatively correlated with DA signals in the SNc, VTA, and DRN during these transitions. Interestingly, the NAc-L and DLS had a strong correlation across all the transition states (Fig. 2, Fig. S2).

Furthermore, during NREM-to-REM transition, peak correlations in DA signals between the PFC and the SNc, VTA, and DRN occurred at t = 0 s, indicating a high degree of synchrony across these regions. In contrast, during the NREM-to-WAKE transition, DA activity in the DRN increased prior to that in the PFC, whereas DA signals in the SNc and VTA rose only after PFC activity increased. DA dynamics in the striatum regions exhibited regional heterogeneity by comparing the correlations with PFC DA signaling during both NREM-to-REM and NREM-to-WAKE transitions. All DA signaling in the NAc-L, NAc-M, and DLS changed after that in the PFC during NREM-to-WAKE transition, and were more synchronized at t = 0 s during NREM-to-REM transition. In the CeA, DA signaling changed later than that in the PFC across all transitions (Fig. 2A, 2C).

Laser-evoked VTA, SNc, and DRN dopamine signaling exhibit distinct response patterns

To map the sources of dopaminergic inputs to key brain regions, including the mPFC, DLS, NAc, and CeA, we employed an integrated approach combining optogenetic activation of dopamine neurons with multi-site fiber photometry recording to monitor real-time dopamine activity. Targeted optogenetic stimulation was achieved using the red-shifted opsin ChrimsonR, enabling precise temporal control of DA neuronal activation while recording. Simultaneous EEG/EMG recordings were conducted to correlate dopamine dynamics with sleep-wake states[19].

Activation of dopamine neurons in the VTA elicited robust dopamine responses in the mPFC, NAc, DLS, and CeA. Notably, the response amplitudes were larger in the NAc and DLS compared to the mPFC and CeA (dopamine responses in the mPFC, NAc, DLS, CeA: 2-s stimulation, mean peak amplitude A = 0.35, 2.04, 1.63, 0.17, respectively. 10-s stimulation: A = 0.36, 1.66, 1.59, 0.20 respectively. Fig. 3A-C). These findings align with the anatomical projections of VTA dopamine neurons[11,20–22], which are denser in the striatum than in the mPFC or CeA[13]. Furthermore, Prolonged optogenetic stimulation was associated with more sustained dopamine responses, indicating a temporal dependence in the response dynamics.

Optogenetic activation of DRN dopamine neurons produced region-specific increases in DA levels within the mPFC, DLS, and CeA (2-s stimulation: mean peak amplitude A = 0.65, 0.21, and 0.10; 10-s stimulation: A = 0.77, 0.29, and 0.29; Fig. 3D–F), in a pattern that mirrors previously described anatomical projections from the DRN to these target regions[12,13].

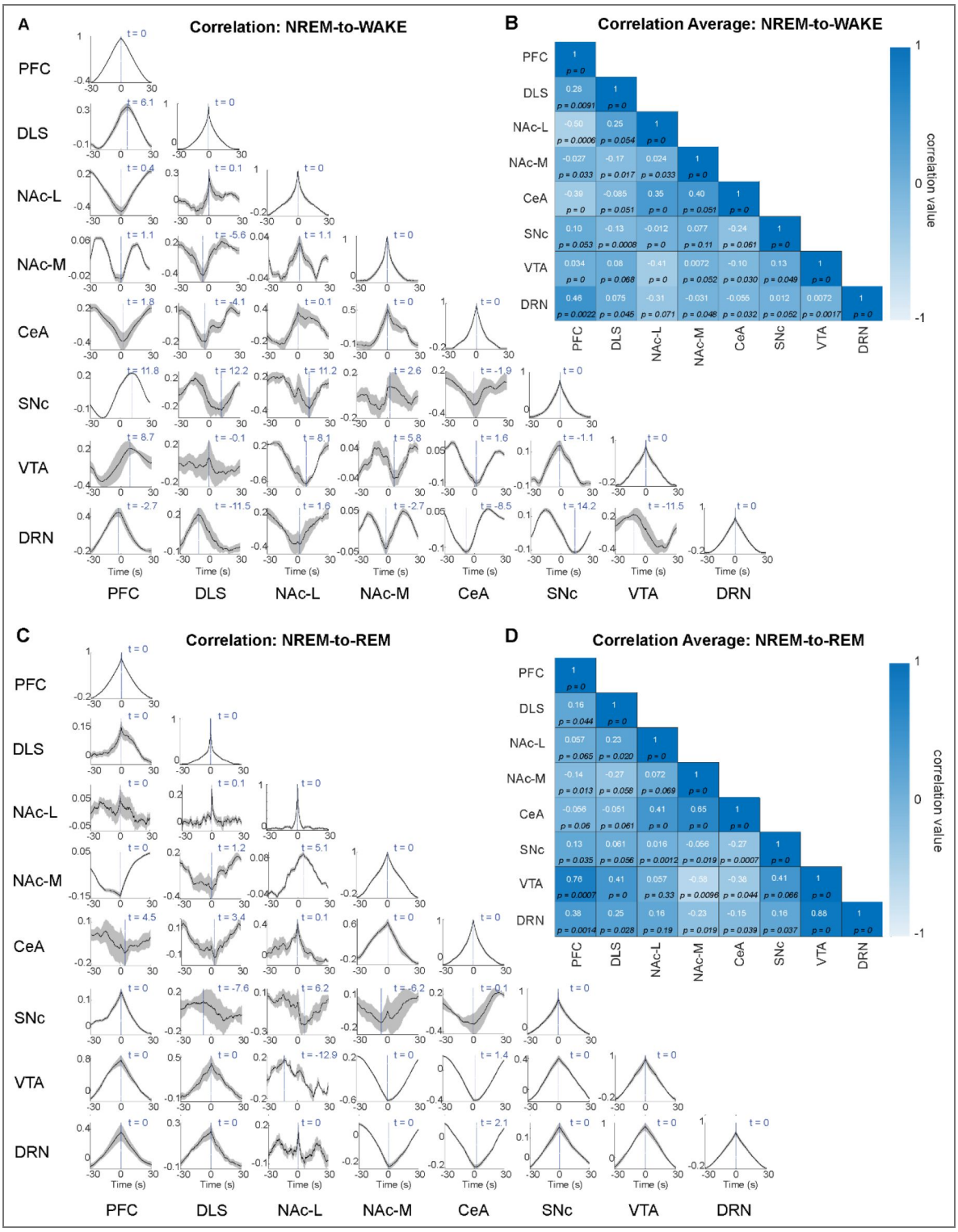

Figure 2. Correlation patterns of dopamine release during sleep-wake transitions.

(A) Temporal correlation of DA signaling during NREM to WAKE transition states between different brain areas recorded simultaneously. **(B)** Correlation coefficient of the DA signals during NREM to WAKE transition states between regions. **(C)** Temporal correlation of DA signaling during NREM to REM transition states between different brain areas recorded simultaneously. **(D)** Correlation coefficient of the DA signals during NREM to REM transition states between regions.

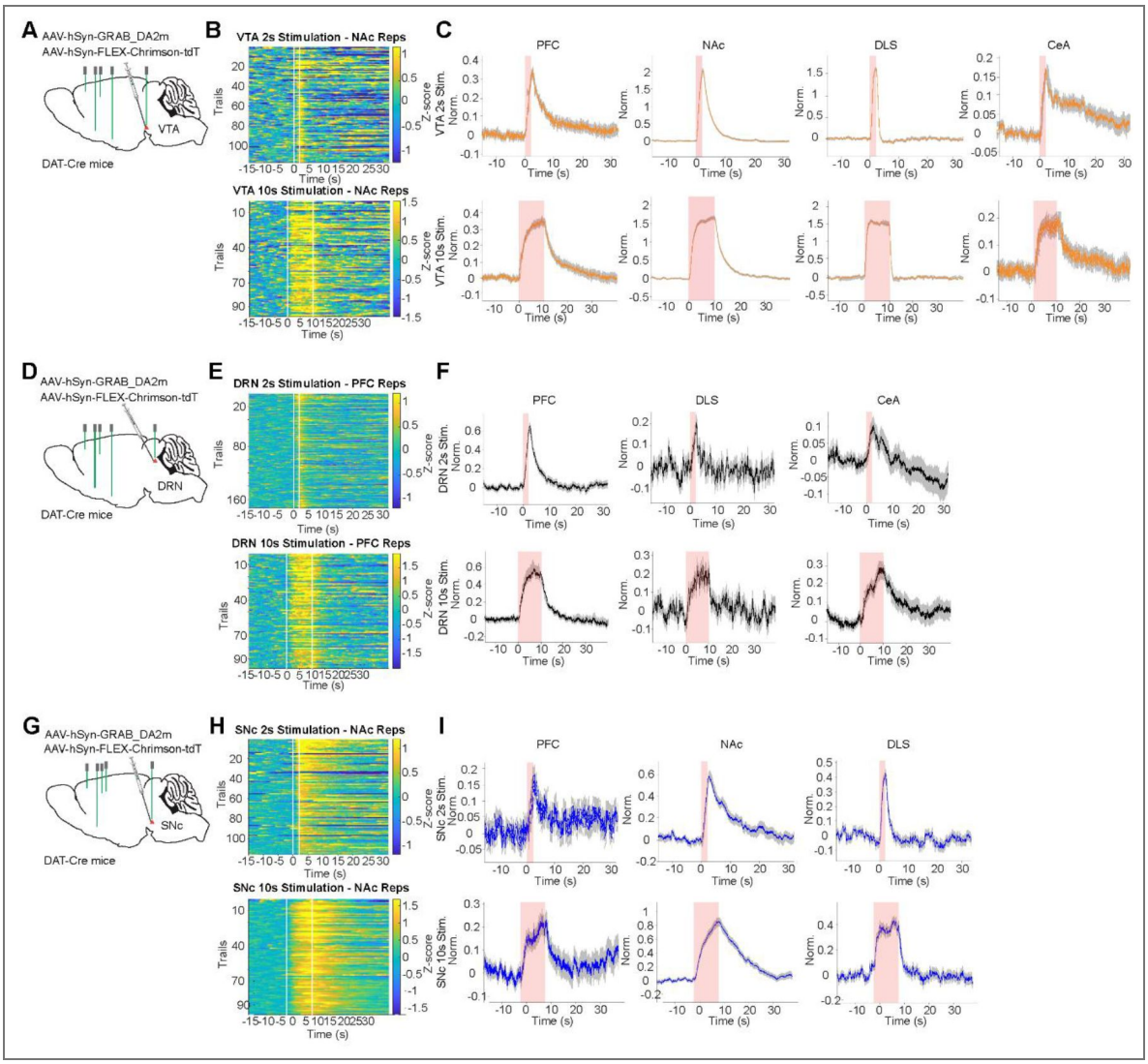

Figure 3. Laser-evoked VTA and DRN dopamine signaling exhibit distinct response patterns.

(A) Schematic illustration depicting the experimental design in which ChrimsonR and GRAB-DA$_{2m}$ vectors were injected into the VTA, and the DA sensor was injected into different downstream targets. **(B)** Heatmap of laser-evoked DA response in NAc in one session. Top, 2 s stimulation protocol; Bottom, 10 s stimulation protocol. **(C)** Laser-evoked DA sensor response in PFC, NAc, DLS, and CeA with the 2 s (averaged peak amplitude: *A* = 0.35, 2.04, 1.63, 0.17 respectively) or 10 s (averaged peak amplitude: *A* = 0.36, 1.66, 1.59, 0.20 respectively) stimulation in the VTA. **(D)** Schematic illustration depicting the experimental design in which ChrimsonR and GRAB-DA$_{2m}$ vectors were injected into the DRN, and the DA sensor was injected into different downstream targets. **(E)** Heatmap of laser-evoked DA response in PFC in one session. Top, 2 s stimulation protocol; Bottom, 10 s stimulation protocol. **(F)** Laser-evoked DA sensor response in PFC, DLS, and CeA with the 2 s (averaged peak amplitude: *A* = 0.65, 0.45, 0.21, 0.10 respectively) or 10 s (averaged peak amplitude: *A* = 0.77, 0.70, 0.29, 0.29 respectively) stimulation in the DRN. **(G)** Schematic illustration depicting the experimental design in which ChrimsonR and GRAB-DA$_{2m}$ vectors were injected into the SNc, and the DA sensor was injected into different downstream targets. **(H)** Heatmap of laser-evoked DA response in NAc in one session. Top, 2 s stimulation protocol; Bottom, 10 s stimulation protocol. **(I)** Laser-evoked DA sensor response in PFC, NAc, and DLS with the 2 s (averaged peak amplitude: *A* = 0.18, 0.57, 0.30, 0.43 respectively) or 10 s (averaged peak amplitude: *A* = 0.24, 0.86, 0.23, 0.44 respectively) stimulation in the SNc.

Consistent with previously described projection patterns[23], activation of SNc dopamine neurons evoked DA responses in the NAc, DLS, and mPFC, with the largest amplitudes observed in the NAc (2-s stimulation: mean peak amplitude A = 0.18, 0.57, and 0.43; 10-s stimulation: A = 0.24, 0.86, and 0.44; Fig. 3G–I).

These widespread responses suggest that dopamine neurons may exert a broad influence across multiple brain areas involved in regulating sleep-wake states and transitions between them.

Activating VTA or DRN but not SNc dopamine neurons promotes wakefulness

To further assess the functional roles of midbrain dopamine source neurons, we expressed a chemogenetic vector *AAV-hSyn-FLEX-Gq* in VTA, SNc, or DRN dopamine neurons of *DAT-Cre* mice and implanted EEG/EMG electrodes to classify brain state changes. In line with prior studies showing that optogenetic activation of VTA dopamine neurons promotes wakefulness[9], we found that CNO-induced activation significantly increased wakefulness while concomitantly reducing both NREM and REM sleep (Fig. 4A, B, G-H). Although both VTA and DRN dopamine neuron activation increased wakefulness and reduced NREM and REM sleep, the effect was more pronounced following VTA activation (Fig. 4C, D, G-H), consistent with prior reports on their roles in arousal regulation[8,9]. Activation of SNc dopamine neurons produced minimal changes in wakefulness and NREM sleep, suggesting a comparatively limited role in arousal regulation (Fig. 4E, F, G-H). Control mice lacking Gq expression showed no significant changes in brain states following CNO injection, confirming the specificity of the chemogenetic manipulation (Fig. S3).

Collectively, these results reveal differential roles of midbrain dopamine neuron subpopulations in in arousal: VTA and DRN dopamine neurons strongly promote wakefulness, whereas SNc dopamine neurons exert comparatively limited influence (Fig. 4G-H).

Discussion

Our study provides a comprehensive brainwide map of dopamine dynamics across sleep-wake transitions, revealing both region-specific and state-specific signatures of DA signaling. Notably, increases in DA levels during transitions from NREM sleep to WAKE were prominent in the mPFC, striatal regions, VTA, SNc, and DRN, consistent with established wake-promoting functions of these dopaminergic circuits[3,8,9,24,25]. However, distinct DA decreases in the CeA and NAc-L during transitions to WAKE, and DA elevations in these regions during NREM to REM transitions, suggest that DA plays specific roles in NREM and REM sleep regulation[15,26,27], contributing to its initiation and maintenance through pathways distinct from those governing wakefulness.

The correlation analyses further support the presence of functional dopaminergic networks. Dopamine signals in amygdalar and nucleus accumbens subregions displayed highly synchronized dynamics, which were negatively correlated with cortical and midbrain DA fluctuations during state transitions. These patterns suggest a functional segregation of dopaminergic signaling— potentially driven by differences in propagation, integration, or local modulation—wherein some circuits are specialized for arousal and others are preferentially engaged during NREM and REM sleep[26–29], which align with prior work implicating VTA, SNc, and DRN DA neurons in sleep-wake regulation[8,9,15,18].

Furthermore, functional differences in DA signaling are likely attributable, at least in part, to regional variations in the kinetics of DA release. To the best of our knowledge, our study provides the first systematic mapping of DA signaling kinetics across key brain regions by selectively stimulating dopaminergic neurons in the SNc, VTA, or DRN. Specific DA responses are also consistent with previous studies that characterized DA signaling from the SNc to striatal subregions[24] and from the VTA to striatal and amygdalar subregions[15,30,31]. Further studies are needed to determine whether specific DA signaling circuits are necessary and/or sufficient to regulate sleep-wake states.

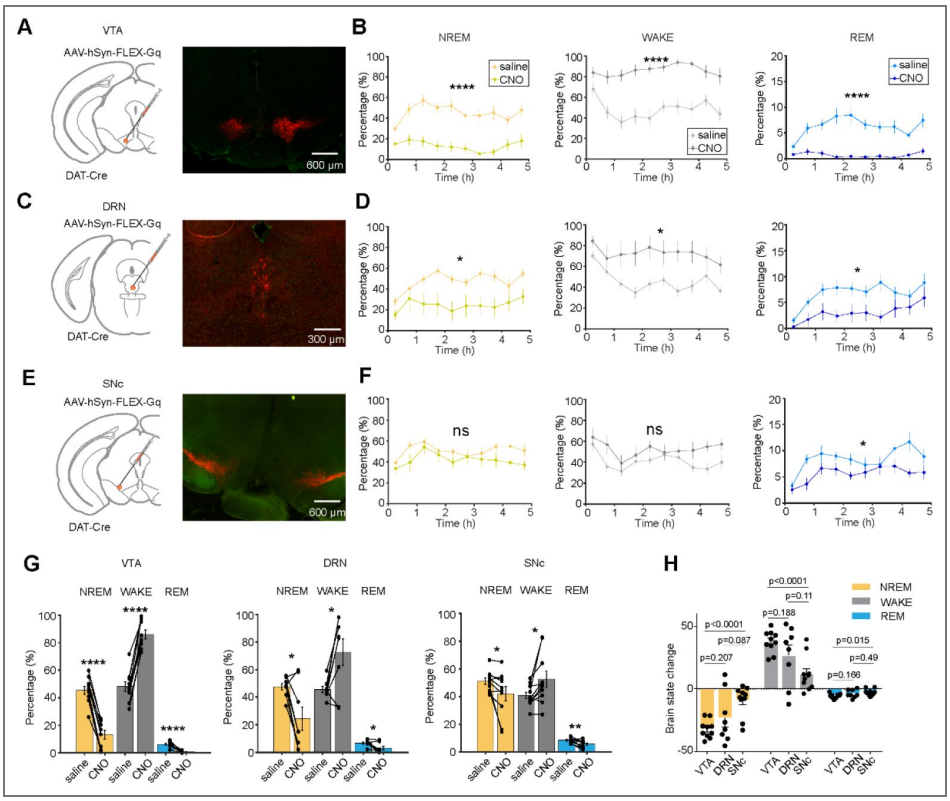

Figure 4. Activating VTA or DRN dopamine neurons promotes wakefulness.

(A) Schematic illustration depicting the experimental design in which Gq vectors were injected into the VTA. The example image shows viral expression in the VTA. **(B)** Effect of VTA DA neurons activation on sleep and wake. Summary of the percentages of time in each brain state following CNO or saline injection in VTA. **(C)** Schematic illustration depicting the experimental design in which Gq vectors were injected into the DRN. The example image shows viral expression in the DRN. **(D)** Effect of DRN DA neurons activation on sleep and wake. Summary of the percentages of time in each brain state following CNO or saline injection in DRN. **(E)** Schematic illustration depicting the experimental design in which Gq vectors were injected into the SNc. The example image shows viral expression in the SNc. **(F)** Effect of SNc DA neurons activation on sleep and wake. Summary of the percentages of time in each brain state following CNO or saline injection in SNc. **(G)** Summary of average percentages of time in each brain state. **(H)** Changes in each brain state induced by chemogenetic activation (difference between CNO and saline injections, averaged across 5 h after injection) in mice with Gq expression in VTA, DRN, or SNc.

Chemogenetic activation of VTA and DRN DA neurons strongly promoted wakefulness, consistent with previous studies using optogenetic activation of VTA[9] and DRN DA neurons[8], respectively. While activation of SNc DA neurons produced only mild effects on sleep-wake states, this may be attributed to the functional heterogeneity of DA neurons within the SNc. Three genetically defined dopamine neuron subtypes—characterized by expression of *Slc17a6*, *Calb1*, and *Anxa1*—have demonstrated significant differences in accelerations and decelerations responses, which may explain the distinct functional profiles of SNc DA neurons in sleep-wake regulation compared to those in the VTA and DRN[25].

Taken together, our results delineate distinct brainwide functional patterns of DA activity during sleep-wake transitions and highlight the complexity of DA-mediated sleep-wake regulations. Future studies are needed to systematically probe how specific DA circuits govern the transitions between different behavioral states.

Materials and Methods

Animals

All procedures were performed in accordance with the protocol approved by the Animal Care and Use Committee at the University of California, Berkeley. Adult (>8 weeks old) male and female Dat-Cre (*Slc6a3*$^{tm1(cre)Xz}$/J. *RRID:IMSR_JAX:020080*) mice were used for all experiments. Mice were kept on a 12:12 light:dark cycle (lights on at 7:00 a.m. and off at 7:00 p.m.) at constant room temperature and humidity with free access to food and water. After Surgeries (virus injections and implantation of EEG/EMG electrodes and optical fibers), mice were individually housed. Recording experiments were conducted 3-5 weeks after surgery.

Surgeries

For all surgeries, anesthesia was induced with 5% isoflurane and maintained with 1.5% isoflurane on a stereotaxic frame. Buprenorphine (0.1 mg/kg) and meloxicam (10 mg/kg) were injected before surgery. Lidocaine (0.5%, 0.1 mL) was injected near the target incision site. The body temperature was kept stable throughout using a heating pad and a feedback thermistor. Eye ointment was applied to keep the eyes from drying. After sterilizing the skin with ethanol and betadine, an incision was made to the skin to expose the skull. Surgeries typically consisted of virus injections followed by EEG/EMG implantation and fiber implantation.

For virus injections, a craniotomy was drilled on the top of the target site, and AAVs were injected into the target regions using a Nanoject II (Drummond Scientific) with glass pipettes. The injection settings were set to a 300 nL injection volume/site at a rate of 23 nL/s with a 15-s interval between injections. pAAV9-hysn-GRAB_DA2m (titer: 2.4 × 10^13 gc/mL, from WZ Biosciences Inc and Addgene) and pAAV-hsyn-GRAB_DA-mut (titer: 2.7 × 10^13 gc/mL, from WZ Biosciences Inc and Addgene) was injected into target sites including:

The medial prefrontal cortex (mPFC): anteroposterior (AP) +1.94 mm, mediolateral (ML) +(/−)0.3 mm, dorsoventral (DV) −2.3–2.5 mm

The nucleus accumbens medial part (NAc-M): AP +1.50 mm, ML +(/−)0.55 mm,DV −4.6–4.8 mm

The nucleus accumbens lateral part (NAc-L): AP +1.42 mm, ML +(/−)1.25 mm, DV −4.6–4.8 mm The Dorsolateral Striatum (DLS): AP +0.98 mm, ML +(/−)2.3 mm, DV −3.0–3.2 mm

The central nucleus of the amygdala (CeA): AP −1.3 mm, ML +(/−)2.6 mm, DV −4.8–4.9 mm

The substantia nigra pars compacta (SNc): AP −3.08 mm, ML +/−1.4 mm, DV −4.1–4.3 mm (bilaterally)

The ventral tegmental area (VTA): AP −3.4 mm, ML +/−0.4 mm, DV −4.3–4.5 mm (bilaterally) The dorsal raphe nucleus (DRN): AP −4.1 mm, ML 0 mm, DV −3.0-3.2 mm

For optogenetic and chemogenetic manipulations, AAV9-hSyn-FLEX-ChrimsonR-tdT (titer: 4.5 × 10^12 gc/mL, from Addgene, or AAV-Ef1a-DIO-rsChRmine-oScarlet-Kv2.1 (titer: 4.8 x 10^12, from UNC Vector Core) and AAV of AAV9-hSyn-DIO-hM3Dq-mCherry (titer: 2× 10^13 gc/mL, from WZ

Biosciences Inc) were injected into SNc, VTA, or DRN. 10 minutes after the virus injection, the injection pipette was slowly removed from the injection site.

For recording the electroencephalogram (EEG) and electromyogram (EMG), stainless-steel wires (0.002” diameter) were soldered to a 20-pin header (Minitek 127T series). EEG screw electrodes were implanted in both sides of the frontal lobe (± 1.5 mm ML, −1.5 mm AP). EMG stainless-steel wire electrodes (0.003” diameter) were inserted into both sides of the trapezius muscle. Reference screws were inserted into each side of the cerebellum. For fiber photometry and optogenetic stimulation, optical fiber implants (1.25-mm ferrule, 200-μm core) were held by a stereotactic fiber holder and slowly implanted into target sites. The EEG/EMG implant was secured by dental cement after fiber implantation.

mPFC: AP +1.94 mm, ML +(/−)0.3 mm, DV −2.5 mm (or angularly 30.38°)

NAc-M: AP +1.50 mm, ML +(/−)0.55 mm, DV −4. 8 mm (or angularly 15.2°)

NAc-L: AP +1.42 mm, ML +(/−)1.25 mm, DV −4. 8 mm

DLS: AP +0.98 mm, ML +(/−)2.3 mm, DV −3. 2 mm (or angularly 14.48°)

CeA: AP −1.3 mm, ML +(/−)2.6 mm, DV −4. 9 mm

SNc: AP −3.08 mm, ML +/−1.4 mm, DV −4.3 mm (bilaterally)

VTA: AP −3.4 mm, ML +/−0.4 mm, DV −4. 5 mm (bilaterally, one fiber was implanted angularly 21. 8°)

DRN: AP −4.1 mm, ML 0 mm, DV −3. 2 mm (or angularly 17.88°)

Fibers were secured with cyanoacrylate glue and dental cement before withdrawing the stereotactic fiber holder.

Sleep recording

Sleep behavioral experiments were carried out in home cages placed in sound-attenuating boxes between 9:00 a.m. and 7:00 p.m. Mice were habituated in the home cages with EEG/EMG cables connected. Each session was recorded for 4–5 h. Each mouse was typically recorded for ≥ 2 sessions. EEG and EMG electrodes were connected to flexible recording cables by a mini-connector. The signals were recorded with a TDT RZ5 amplifier (Synapse software), filtered (0– 300 Hz) and digitized at 1,500 Hz. Spectral analysis was carried out using fast Fourier transform (FFT). For each 5-s epoch, the brain state was classified into NREM, REM or wake states on the basis of EEG and EMG data (wake: desynchronized EEG and high EMG activity; NREM: synchronized EEG with high-amplitude, low-frequency (0.5–4 Hz) activity and low EMG activity; REM: high power at theta frequencies (6–9 Hz) and low EMG activity). Consecutive epochs of the same state were combined into a single episode. The classification was performed semi-automatically using a custom-written graphical user interface (programmed in MATLAB 2022a, MathWorks). For the comparison of normalized EEG power spectra within each brain state, the EEG spectra were normalized to the total EEG power between 0 and 25 Hz.

Optogenetic stimulation

To study the laser evoked responses of dopamine release or sleep behavior changes induced by activation of either VTA or DRN dopamine neurons, we applied laser stimulation (635 nm, 10-mW at fiber tip). For laser evoked responses of dopamine release, two stimulation protocols were applied: (1), 30 Hz (10 ms pulse) with 2 seconds epochs for 2h stimulations, the inter-stimulation-interval was 1 minute between epochs. (2), 30 Hz (10 ms pulse) with 10 seconds epochs for 2h stimulations, the inter-stimulation-interval was 1 minute between epochs. Mice were recorded for 1h as baseline, and recorded 1h more post-stimulation.

Chemogenetic manipulation

For chemogenetic manipulation, saline (0.9% sodium chloride) or CNO (C0832, Sigma; dissolved in saline) was injected i.p. into mice expressing hM3Dq or mice without hM3Dq expression. The CNO dose was 1 mg kg−1 body weight for hM3Dq or control experiments. Each recording session

started immediately after injection and lasted for 5 h. Each mouse was recorded for 6–8 sessions, and CNO was given randomly in half of the sessions, while saline was given in the other half. Data was averaged across all sessions.

Fiber photometry recording

Fiber photometry was performed using a Multichannel Fiber Photometry System (R820, RWD Life Science), with 470 nm and 410 nm LEDs. The sampling rate for each channel was 30 frames/s. The system was synchronized with TDT sleep recording system by TTL pulses. For analysis of GRABDA2m signals, we fit the 470 and 410 nm channels to a bi-exponential decay function to approximate the slow photobleaching time course. The bi-exponential fit was subtracted from each channel, and the 410 nm channel was fit to the 470 nm channel using a least squares method. The final corrected 470-nm signal was z-scored for further analysis.

Histology

To evaluate the location and strength of virus expression as well as the fiber position, mice were anesthetized with isoflurane before transcardial perfusion with 20 mL 1× PBS (Gibco) and 20 mL 4% paraformaldehyde (Electron Microscopy Sciences) in 1× PBS. For fiber localization, the mouse head with implants was fixed in 4% paraformaldehyde for >24h before separating the brain from the top of the skull. Then the brain was tripped out from the skull, and further fixed with 4% paraformaldehyde for 24h. The fixed brain was dehydrated in 20 mL of 30% sucrose PBS for 24 h, allowing time for it to sink to the bottom of a conical tube. The brain was then embedded in tissue freezing medium (General Data Company, Inc.) and frozen for at least half an hour. The brain was cryosectioned at 40 μm using a cryostat (Leica). Slides were then imaged on a fluorescence microscope (Keyence).

Statistical analysis

All statistical analyses were performed using MATLAB v2022a (MathWorks) and Prism9 v4.0 (GraphPad). All statistical comparisons were conducted on animals. The number of mice and the level of significance are indicated in the figure legends. Two-group comparisons were performed using a t-test. Multiple group comparisons were performed using either two-way or one-way ANOVA, following multiple two-group tests with α correction, adjusting for multiple comparisons. All statistics are reported as the mean ± s.e.m.

Data availability

All data and code for this paper are available upon request.

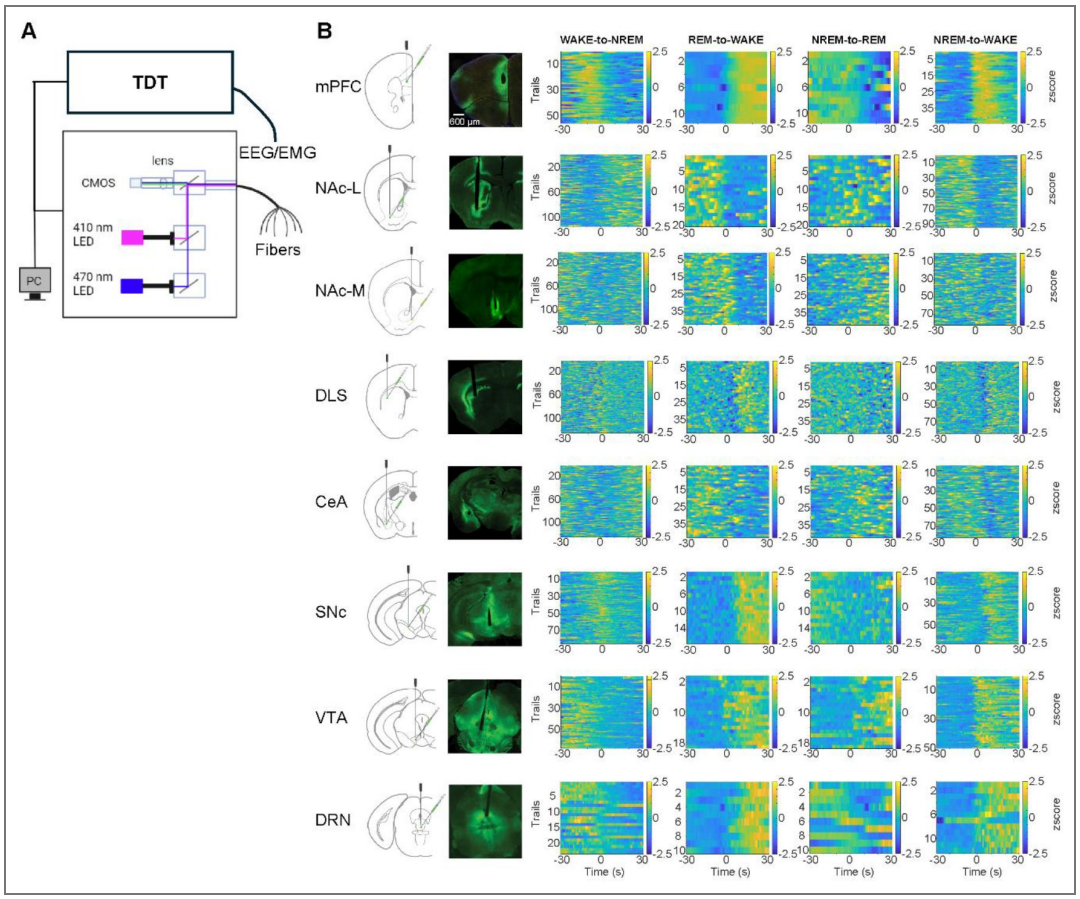

Supplemental Figure 1. Dopamine dynamics across brain-state transitions in distinct brain regions. (A) Schematic of multi-site fiber photometry and EEG/EMG recording. TDT, Tucker-Davis Technologies. **(B)** Example of DA dynamics across different brain-state transitions. For each row: Left, Schematic of DA sensor injection; middle, example image of DA sensor expression; right, heatmap of DA signal across different transitions.

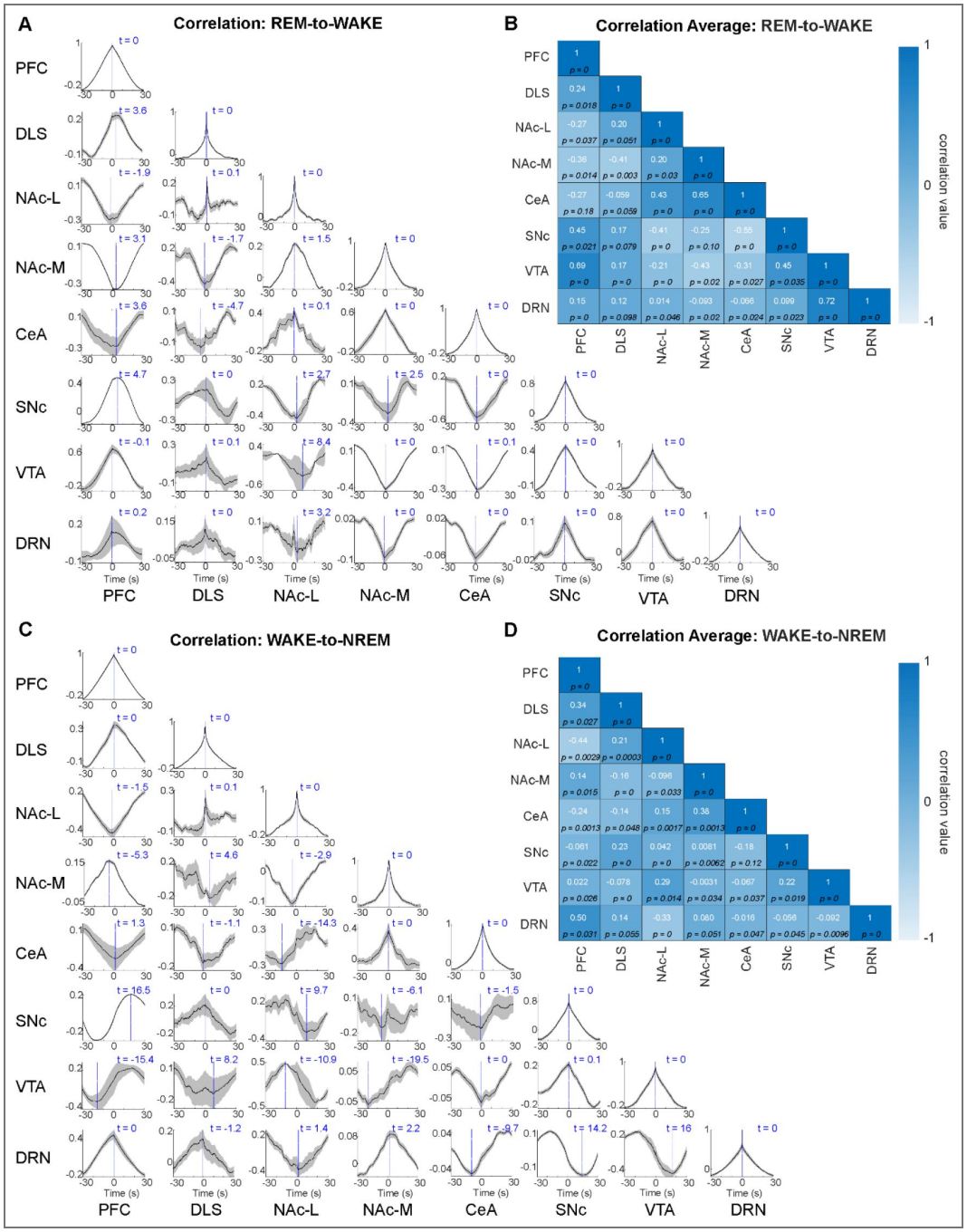

Supplemental Figure 2. Correlation patterns of dopamine release during sleep-wake transitions.

(A) Temporal correlation of DA signaling during REM to WAKE transition states between different brain areas recorded simultaneously. **(B)** Correlation coefficient of the DA signals during REM to WAKE transition states between regions. **(C)** Temporal correlation of DA signaling during WAKE to NREM transition states between different brain areas recorded simultaneously. **(D)** Correlation coefficient of the DA signals during WAKE to NREM transition states between regions.

Supplemental Figure 3. Control experiment for chemogenetic activation.

(A) Schematic of EEG/EMG recording in mice without Gq vectors expression. **(B)** Summary of the percentages of time in each brain state following CNO or saline injection in DRN. **(C)** Summary of averaged percentages of time in each brain state.

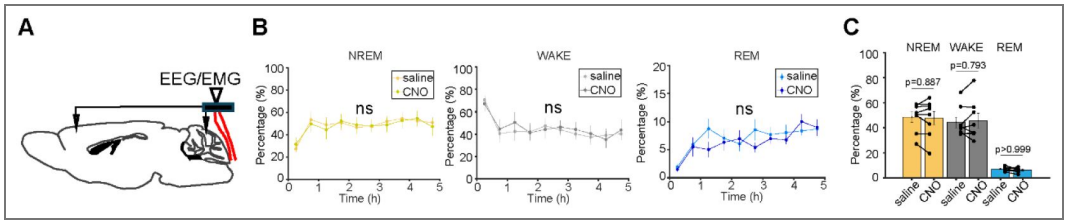

Supplemental Table.

Figure #	Conditions	n per group	Analysis	Factor	P value	P value summary
1C	PFC	29	One-way ANOVA with multiple comparisons	WAKE vs NREM	< 0.0001	****
				WAKE vs REM	< 0.0001	****
				NREM vs REM	0.0006	***
	NAc-L	9	One-way ANOVA with multiple comparisons	WAKE vs NREM	0.0005	***
				WAKE vs REM	0.0019	**
				NREM vs REM	0.96	ns
	NAc-M	5	One-way ANOVA with multiple comparisons	WAKE vs NREM	0.79	ns
				WAKE vs REM	< 0.0001	****
				NREM vs REM	< 0.0001	****
	DLS	37	One-way ANOVA with multiple comparisons	WAKE vs NREM	0.25	ns
				WAKE vs REM	< 0.0001	****
				NREM vs REM	< 0.0001	****
	DMS	4	One-way ANOVA with multiple comparisons	WAKE vs NREM	0.99	ns
				WAKE vs REM	0.19	ns
				NREM vs REM	0.15	ns
	CeA	11	One-way ANOVA with multiple comparisons	WAKE vs NREM	0.094	ns
				WAKE vs REM	< 0.0001	****
				NREM vs REM	0.0048	**
	SNc	6	One-way ANOVA with multiple comparisons	WAKE vs NREM	0.6	ns
				WAKE vs REM	0.0086	**
				NREM vs REM	0.059	ns
	VTA	5	One-way ANOVA with multiple comparisons	WAKE vs NREM	0.64	ns
				WAKE vs REM	0.0038	**
				NREM vs REM	0.017	*
	DRN	14	One-way ANOVA with multiple comparisons	WAKE vs NREM	0.67	ns
				WAKE vs REM	0.44	ns
				NREM vs REM	0.91	ns
4B	NREM	10, 10	Two-way ANOVA	saline vs CNO	< 0.0001	****
	WAKE	10, 10	Two-way ANOVA	saline vs CNO	< 0.0001	****
	REM	10, 10	Two-way ANOVA	saline vs CNO	< 0.0001	****
4D	NREM	8, 8	Two-way ANOVA	saline vs CNO	0.0204	*
	WAKE	8, 8	Two-way ANOVA	saline vs CNO	0.0168	*
	REM	8, 8	Two-way ANOVA	saline vs CNO	0.0213	*
4F	NREM	10, 10	Two-way ANOVA	saline vs CNO	0.1319	ns
	WAKE	10, 10	Two-way ANOVA	saline vs CNO	0.0812	ns
	REM	10, 10	Two-way ANOVA	saline vs CNO	0.0158	*
4G	NREM	10, 10	Paired t test	saline vs CNO	< 0.0001	****
	WAKE	10, 10	Paired t test	saline vs CNO	< 0.0001	****
	REM	10, 10	Paired t test	saline vs CNO	< 0.0001	****
4H	NREM	8, 8	Paired t test	saline vs CNO	0.0159	*
	WAKE	8, 8	Paired t test	saline vs CNO	0.0147	*
	REM	8, 8	Paired t test	saline vs CNO	0.0132	*
4I	NREM	10, 10	Paired t test	saline vs CNO	0.0414	*
	WAKE	10, 10	Paired t test	saline vs CNO	0.0254	*
	REM	10, 10	Paired t test	saline vs CNO	0.0079	**
4J	NREM	10, 8	Unpaired t test	VTA vs DRN	0.2067	ns
	NREM	10, 10	Unpaired t test	VTA vs SNC	< 0.0001	****
	NREM	8, 10	Unpaired t test	DR vs SNC	0.0869	ns
	WAKE	10, 8	Unpaired t test	VTA vs DRN	0.1884	ns
	WAKE	10, 10	Unpaired t test	VTA vs SNC	< 0.0001	****
	WAKE	8, 10	Unpaired t test	DR vs SNC	0.1098	ns
	REM	10, 8	Unpaired t test	VTA vs DRN	0.1657	ns
	REM	10, 10	Unpaired t test	VTA vs SNC	0.0146	*
	REM	8, 10	Unpaired t test	DR vs SNC	0.4905	ns
S3B	NREM	8, 8	Two-way ANOVA	saline vs CNO	0.3672	ns
	WAKE	8, 8	Two-way ANOVA	saline vs CNO	0.331	ns
	REM	8, 8	Two-way ANOVA	saline vs CNO	0.3066	ns
S3C	NREM	8, 8	Tukey's multiple comparisons test	saline vs CNO	0.8868	ns
	WAKE	8, 8	Tukey's multiple comparisons test	saline vs CNO	0.7928	ns
	REM	8, 8	Tukey's multiple comparisons test	saline vs CNO	> 0.9999	ns

Acknowledgements

We sincerely thank Prof. Yang Dan for her invaluable support, including funding, laboratory space, equipment, and exceptional guidance and supervision throughout this work. We thank Dr. Daniel Silverman for providing some photometry analysis code. We also appreciate the administrative assistance provided by Dr. Hongfeng Gao. Additionally, we are grateful to all members of the Dan Lab for their insightful discussions and collaborative support.

Additional information

Funding

This work was supported by Howard Hughes Medical Institute investigator (Y. D.).

Author contributions

Conceptualization: C.C., X.T., and L.L. Methodology: C.C., X.T., L.L. Investigation: C.C., X.T., L.L., C.P., X.Z., R.S., E.L., Z.J., W.C., Y.Y., M.K., K.B.H., D.D., and D.S. Data analysis: C.C., X.T., L.L. Writing, review, and editing: C.C., X.T., and L.L.

Funding

Funder	Grant reference number	Author
Howard Hughes Medical Institute (HHMI)		Xun Tu
Howard Hughes Medical Institute (HHMI)		Lihui Lu
Howard Hughes Medical Institute (HHMI)		Changwan Chen

Author ORCID iDs

Changwan Chen: https://orcid.org/0000-0002-2520-8516
Xiaofan Zhang: https://orcid.org/0009-0008-6668-0690

References

(1) **Monti J. M.,** Monti D. (2007) The Involvement of Dopamine in the Modulation of Sleep and Waking. *Sleep Med. Rev* **11**:113-133 https://doi.org/10.1016/j.smrv.2006.08.003 | PubMed

(2) **Saper C. B.,** Fuller P. M., Pedersen N. P., Lu J., Scammell T. E. (2010) Sleep State Switching. *Neuron* **68**:1023-1042 https://doi.org/10.1016/j.neuron.2010.11.032 | PubMed

(3) **Liu D.,** Dan Y. (2019) A Motor Theory of Sleep-Wake Control: Arousal-Action Circuit. *Annu. Rev. Neurosci* **42**:27-46 https://doi.org/10.1146/annurev-neuro-080317-061813 | PubMed

(4) **Ma C.,** Dan Y. (2025) The How and Why of Sleep: Motor Theory and Catecholamine Hypothesis. *Neuron* **113**:3315-3332 https://doi.org/10.1016/j.neuron.2025.08.017 | PubMed

(5) **Gerfen C. R.,** Surmeier D. J. (2011) Modulation of Striatal Projection Systems by Dopamine. *Annu. Rev. Neurosci* **34**:441-466 https://doi.org/10.1146/annurev-neuro-061010-113641 | PubMed

(6) **Watabe-Uchida M.,** Zhu L., Ogawa S. K., Vamanrao A., Uchida N. (2012) Whole-Brain Mapping of Direct Inputs to Midbrain Dopamine Neurons. *Neuron* **74**:858-873 https://doi.org/10.1016/j.neuron.2012.03.017 | PubMed

(7) **Beier K. T.,** Steinberg E. E., DeLoach K. E., Xie S., Miyamichi K., Schwarz L., Gao X. J., Kremer E. J., Malenka R. C., Luo L. (2015) Circuit Architecture of VTA Dopamine Neurons Revealed by Systematic Input-Output Mapping. *Cell* **162**:622-634 https://doi.org/10.1016/j.cell.2015.07.015 | PubMed

(8) **Cho J. R.,** Treweek J. B., Robinson J. E., Xiao C., Bremner L. R., Greenbaum A., Gradinaru V. (2017) Dorsal Raphe Dopamine Neurons Modulate Arousal and Promote Wakefulness by Salient Stimuli. *Neuron* **94**:1205-1219.e8. https://doi.org/10.1016/j.neuron.2017.05.020 | PubMed

(9) **Eban-Rothschild A.,** Rothschild G., Giardino W. J., Jones J. R., de Lecea L. (2016) VTA Dopaminergic Neurons Regulate Ethologically Relevant Sleep–Wake Behaviors. *Nat. Neurosci* **19**:1356-1366 https://doi.org/10.1038/nn.4377 | PubMed

(10) **Chen C.,** Altafi M., Corbu M.-A., Trenk A., van den Munkhof H., Weineck K., Bender F., Carus-Cadavieco M., Bakhareva A., Korotkova T., *et al.* (2024) The Dynamic State of a Prefrontal–Hypothalamic–Midbrain Circuit Commands Behavioral Transitions. *Nat. Neurosci* **27**:952-963 https://doi.org/10.1038/s41593-024-01598-3 | PubMed

(11) **Beier K. T.,** Steinberg E. E., DeLoach K. E., Xie S., Miyamichi K., Schwarz L., Gao X. J., Kremer E. J., Malenka R. C., Luo L. (2015) Circuit Architecture of VTA Dopamine Neurons Revealed by Systematic Input-Output Mapping. *Cell* **162**:622-634 https://doi.org/10.1016/j.cell.2015.07.015 | PubMed

(12) **Lin R.,** Liang J., Wang R., Yan T., Zhou Y., Liu Y., Feng Q., Sun F., Li Y., Li A., *et al.* (2020) The Raphe Dopamine System Controls the Expression of Incentive Memory. *Neuron* **0** https://doi.org/10.1016/j.neuron.2020.02.009 | PubMed

(13) **Oh S. W.,** Harris J. A., Ng L., Winslow B., Cain N., Mihalas S., Wang Q., Lau C., Kuan L., Henry A. M., *et al.* (2014) A Mesoscale Connectome of the Mouse Brain. *Nature* **508**:207-214 https://doi.org/10.1038/nature13186 | PubMed

(14) **Björklund A.,** Dunnett S. B. (2007) Dopamine Neuron Systems in the Brain: An Update. *Trends Neurosci* **30**:194-202 https://doi.org/10.1016/j.tins.2007.03.006 | PubMed

(15) **Hasegawa E.,** Miyasaka A., Sakurai K., Cherasse Y., Li Y., Sakurai T. (2022) Rapid Eye Movement Sleep Is Initiated by Basolateral Amygdala Dopamine Signaling in Mice. *Science* **375**:994-1000 https://doi.org/10.1126/science.abl6618 | PubMed

(16) **Summa K. C.,** Jiang P., González-Rodríguez P., Huang X., Lin X., Vitaterna M. H., Dan Y., Surmeier D. J., Turek F. W. (2024) Disrupted Sleep-Wake Regulation in the MCI-Park Mouse Model of Parkinson's Disease. *Npj Park Dis* **10**:54 https://doi.org/10.1038/s41531-024-00670-w | PubMed

(17) **Sun F.,** Zhou J., Dai B., Qian T., Zeng J., Li X., Zhuo Y., Zhang Y., Wang Y., Qian C., *et al.* (2020) Next-Generation GRAB Sensors for Monitoring Dopaminergic Activity in Vivo. *Nat. Methods* **17**:1156-1166 https://doi.org/10.1038/s41592-020-00981-9 | PubMed

(18) **Toth B. A.,** Chang K. S., Fechtali S., Burgess C. R. (2023) Dopamine Release in the Nucleus Accumbens Promotes REM Sleep and Cataplexy. *iScience* **26**:107613 https://doi.org/10.1016/j.isci.2023.107613 | PubMed

(19) **Silverman D.,** Chen C., Chang S., Bui L., Zhang Y., Raghavan R., Jiang A., Le A., Darmohray D., Sima J., *et al.* (2025) Activation of Locus Coeruleus Noradrenergic Neurons Rapidly Drives Homeostatic Sleep Pressure. *Sci. Adv* **11**:eadq0651 https://doi.org/10.1126/sciadv.adq0651 | PubMed

(20) **Menegas W.,** Bergan J. F., Ogawa S. K., Isogai Y., Umadevi Venkataraju K., Osten P., Uchida N., Watabe-Uchida M. (2015) Dopamine Neurons Projecting to the Posterior Striatum Form an Anatomically Distinct Subclass. *eLife* **4**:e10032 https://doi.org/10.7554/eLife.10032 | PubMed

(21) **Mininni C. J.,** Caiafa C. F., Zanutto B. S., Tseng K. Y., Lew S. E. (2018) Putative Dopamine Neurons in the Ventral Tegmental Area Enhance Information Coding in the Prefrontal Cortex. *Sci. Rep* **8**:11740 https://doi.org/10.1038/s41598-018-29979-2 | PubMed

(22) **Huang S.,** Zhang Z., Gambeta E., Xu S. C., Thomas C., Godfrey N., Chen L., M'Dahoma S., Borgland S. L., Zamponi G. W. (2020) Dopamine Inputs from the Ventral Tegmental Area into the Medial Prefrontal Cortex Modulate Neuropathic Pain-Associated Behaviors in Mice. *Cell Rep* **31**:107812 https://doi.org/10.1016/j.celrep.2020.107812 | PubMed

(23) **Lerner T. N.,** Shilyansky C., Davidson T. J., Evans K. E., Beier K. T., Zalocusky K. A., Crow A. K., Malenka R. C., Luo L., Tomer R., *et al.* (2015) Intact-Brain Analyses Reveal Distinct Information Carried by SNc Dopamine Subcircuits. *Cell* **162**:635-647 https://doi.org/10.1016/j.cell.2015.07.014 | PubMed

(24) **Howe M. W.,** Dombeck D. A. (2016) Rapid Signalling in Distinct Dopaminergic Axons during Locomotion and Reward. *Nature* **535**:505-510 https://doi.org/10.1038/nature18942 | PubMed

(25) **Azcorra M.,** Gaertner Z., Davidson C., He Q., Kim H., Nagappan S., Hayes C. K., Ramakrishnan C., Fenno L., Kim Y. S., *et al.* (2023) Unique Functional Responses Differentially Map onto Genetic Subtypes of Dopamine Neurons. *Nat. Neurosci* **26**:1762-1774 https://doi.org/10.1038/s41593-023-01401-9 | PubMed

(26) **Ma C.,** Zhong P., Liu D., Barger Z. K., Zhou L., Chang W.-C., Kim B., Dan Y. (2019) Sleep Regulation by Neurotensinergic Neurons in a Thalamo-Amygdala Circuit. *Neuron* **103**:323-334.e7 https://doi.org/10.1016/j.neuron.2019.05.015 | PubMed

(27) **Oishi Y.,** Xu Q., Wang L., Zhang B.-J., Takahashi K., Takata Y., Luo Y.-J., Cherasse Y., Schiffmann S. N., de Kerchove d'Exaerde A., *et al.* (2017) Slow-Wave Sleep Is Controlled by a Subset of Nucleus Accumbens Core Neurons in Mice. *Nat. Commun* **8**:734 https://doi.org/10.1038/s41467-017-00781-4 | PubMed

(28) **Kato T.,** Tanaka K. F., Natsubori A. (2023) Dopamine Receptor Type 2-Expressing Medium Spiny Neurons in the Ventral Lateral Striatum Have a Non-REM Sleep-Induce Function. *eNeuro* **10** https://doi.org/10.1523/ENEURO.0327-23.2023 | PubMed

(29) **Yuan X.-S.,** Wang L., Dong H., Qu W.-M., Yang S.-R., Cherasse Y., Lazarus M., Schiffmann S. N., d'Exaerde A. de K., Li R.-X., *et al.* (2017) Striatal Adenosine A2A Receptor Neurons Control Active-Period Sleep via Parvalbumin Neurons in External Globus Pallidus. *eLife* **6**:e29055 https://doi.org/10.7554/eLife.29055 | PubMed

(30) **Zheng Y.,** Cai R., Wang K., Zhang J., Zhuo Y., Dong H., Zhang Y., Wang Y., Deng F., Ji E., *et al.* (2025) In Vivo Multiplex Imaging of Dynamic Neurochemical Networks with Designed Far-Red Dopamine Sensors. *Science* **388**:eadt7705 https://doi.org/10.1126/science.adt7705

(31) **Li L.,** Lu L., Ren Y., Tang G., Zhao Y., Cai X., Shi Z., Ding H., Liu C., Cheng D., *et al.* (2022) Colocalized, Bidirectional Optogenetic Modulations in Freely Behaving Mice with a Wireless Dual-Color Optoelectronic Probe. *Nat. Commun* **13**:839 https://doi.org/10.1038/s41467-022-28539-7 | PubMed

Peer reviews

Reviewer #1 (Public review):

Summary:

In this manuscript, Chen, Tu, and Lu focused on how brain-wide dopamine release dynamically changes during sleep/wake state transitions. Using multi-site fiber photometry to monitor DA release, alongside simultaneous EEG and EMG recordings, the authors show distinct DA dynamics during transitions from NREM to WAKE, REM to WAKE, WAKE to NREM, and NREM to REM. Next, they analyze temporal coordination between regions using cross-correlation analysis. Finally, chemogenetic activation of VTA or DRN but not SNc dopamine neurons is shown to promote wakefulness.

Strengths:

The manuscript addresses an interesting question: how brainwide dopamine activity evolves across sleep/wake transitions. The combination of multi-site DA recordings with simultaneous EEG/EMG monitoring is technically sophisticated. The experimental logic is generally clear, and the dataset is rich. The result has several interesting observations.

Weaknesses:

The authors used the GRAB-DA2m sensor to monitor dopamine release. Although DA2m exhibits higher affinity for dopamine compared to NE (around 15-fold difference in EC50 in HEK cell assays), it is still possible that NE contributes to the recorded signals, particularly during sleep/wake transitions when locus coeruleus activity is strongly modulated. Given the widespread and state-dependent dynamics of NE, this potentially needs to be addressed.

Similarly, the chemogenetic experiments rely on CNO to activate hM3Dq-expressing dopamine neurons. However, it is well established that CNO can be converted to clozapine in rodents, and clozapine itself is known to influence sleep/wake. Although the authors included non-hM3Dq-expressing mice as controls, the potential confounding effects of clozapine on sleep regulation remain a concern.

Midbrain dopamine neurons exhibit both tonic and phasic firing patterns. In Figure 1, most reported dopamine transitions appear relatively slow. However, some faster, phasic-like components are observable. For example, in NAc-L during REM-to-WAKE transitions, there are 2 phasic-like decreases between −20 and 0 s. The authors used laser-evoked stimulation experiments in the VTA and DRN and showed that 2 s versus 10 s stimulation produces distinct dopamine kinetics, suggesting that different firing patterns generate distinct DA dynamics. Moreover, the temporal profiles vary not only across regions but also across transitions within the same region. For example, in CeA, the NREM-to-WAKE transition shows a relatively rapid decrease, whereas REM-to-WAKE displays a much slower decline. Similarly, some regions (e.g., NAc-L NREM-to-WAKE, DRN REM-to-WAKE) show faster changes, while others (e.g., mPFC WAKE-to-NREM, VTA NREM-to-WAKE) show slower kinetics. These observations argue against a simple region-specific explanation and instead suggest that distinct firing modes may differentially contribute depending on transition type.

While cross-correlation analysis provides insight into the temporal coordination of DA signals across regions, several limitations should be considered. Sleep/wake transitions are inherently non-stationary events, whereas cross-correlation assumes relatively stable signal properties within the analysis window. This mismatch may bias lag estimates and obscure transient lead-lag relationships. Moreover, the temporal resolution of fiber photometry and the kinetics of genetically encoded DA sensors limit the precision with which timing relationships can be interpreted, particularly for sub-second lags.

In the Introduction, the authors state that they aim to address 'which dopaminergic populations causally drive these patterns.' However, the chemogenetic approach used operates on a relatively slow timescale: CNO-induced activation takes 15-30 minutes to produce effects, and the induced changes are long-lasting. In contrast, the dopamine transitions described in Figure 1 occur on a much faster timescale compared to CNO manipulation. Thus, while chemogenetic activation demonstrates that stimulating VTA or DRN dopamine neurons promotes wakefulness, it does not directly establish that these populations causally drive the rapid transition-related DA dynamics observed in the photometry recordings.

https://doi.org/10.7554/eLife.110675.1.sa2

Reviewer #2 (Public review):

In "Brainwide dopamine dynamics across sleep-wake transitions", Chen et al. provide a thorough description of how dopamine dynamics fluctuate across sleep-wake transitions and in transitions between sleep states. To achieve this, the authors used multi-channel fiber photometry and a genetically encoded fluorescent dopamine reporter to simultaneously measure dopamine dynamics in 8 brain regions. They also used EEG measurements to precisely quantify and time transitions between sleep states and wakefulness. Finally, the authors used channelrhodopsin to examine dopamine dynamics following subregion stimulation and chemogenetics to test the causal relationship between activation of distinct dopamine neuron populations and their effects on sleep state.

The conclusions made by the authors in this study are modest and appropriate given the largely observational nature of the principal findings. The use of optogenetics to probe regional dopamine signaling following activation of distinct nuclei is interesting, but not

entirely novel and constrained in interpretability. Similarly, the chemogenetics experiment largely confirms previous studies, which the authors correctly cited in the text.

The principal findings of this study are based on strong methodological and analytical methods. Implanting 8 optical fibers in a single mouse, along with EEG/EMG electrodes, is technically challenging, providing valuable, simultaneous measurements of dopamine fluctuations across the brain. This enables the strong correlational and time-locked analyses performed by the authors in Figure 2. What's more, the use of EEG/EMG electrodes provides time-locked descriptions of sleep states, enabling precise comparisons between the dopamine signal and sleep state transitions.

The paper has some weaknesses that the authors could address. The analyses in Figure 1 could be strengthened to show how dopamine changes during transitions between specific sleep states. The injection sites for channelrhodopsin and chemogenetic viruses could be validated to strengthen the interpretation of those results. Also, a stronger justification for the experiments conducted in Figure 3 could be provided, as they seem unrelated to the present study.

Overall, this study has strong descriptive power, convincingly showing how dopamine fluctuates across sleep states. Some of the other aspects of the paper, however, are somewhat limited in novelty and interpretation.

https://doi.org/10.7554/eLife.110675.1.sa1

Author response:

> ***Public Reviews:***
>
> ***Reviewer #1 (Public review):***
>
> *Summary:*
>
> *In this manuscript, Chen, Tu, and Lu focused on how brain-wide dopamine release dynamically changes during sleep/wake state transitions. Using multi-site fiber photometry to monitor DA release, alongside simultaneous EEG and EMG recordings, the authors show distinct DA dynamics during transitions from NREM to WAKE, REM to WAKE, WAKE to NREM, and NREM to REM. Next, they analyze temporal coordination between regions using cross-correlation analysis. Finally, chemogenetic activation of VTA or DRN but not SNc dopamine neurons is shown to promote wakefulness.*
>
> *Strengths:*
>
> *The manuscript addresses an interesting question: how brainwide dopamine activity evolves across sleep/wake transitions. The combination of multi-site DA recordings with simultaneous EEG/EMG monitoring is technically sophisticated. The experimental logic is generally clear, and the dataset is rich. The result has several interesting observations.*
>
> *Weaknesses:*
>
> *The authors used the GRAB-DA2m sensor to monitor dopamine release. Although DA2m exhibits higher affinity for dopamine compared to NE (around 15-fold difference in EC50 in HEK cell assays), it is still possible that NE contributes to the recorded signals, particularly during sleep/wake transitions when locus coeruleus activity is strongly modulated. Given the widespread and state-dependent dynamics of NE, this potentially needs to be addressed.*

We thank the reviewer for raising this important methodological consideration. While we acknowledge that a minor contribution from norepinephrine (NE) to the DA2m signal cannot

be categorically excluded, several convergent lines of evidence give us confidence that the signals we recorded primarily reflect dopamine release.

First, DA2m has substantially lower affinity for NE compared to dopamine. The reported EC_{50} for NE is ~1200 nM [1], which is ~15-fold higher than for dopamine. In contrast, extracellular NE levels in the prefrontal cortex are typically in the low nanomolar range (generally <5 nM under basal conditions) [2,3]. Because physiological NE concentrations are orders of magnitude below the sensor's EC_{50} threshold, NE is highly unlikely to drive significant DA2m activation *in vivo*.

Second, our optogenetic experiments provide direct functional validation. The targeted stimulation of midbrain dopaminergic neurons elicited robust DA2m signal responses across both cortical and subcortical brain areas. This confirms that the sensor reliably captures evoked dopamine release within our specific experimental paradigm.

Finally, the spontaneous DA2m signal dynamics we observed across sleep-wake states functionally diverge from previously reported patterns of cortical NE release [4]. For example, in Figure 1C, our DA2m recordings in the mPFC revealed high activity during wakefulness, alongside pronounced, sharp changes during NREM-to-WAKE transitions. In contrast, prior study [4] show that NE exhibits comparatively mild fluctuations during wakefulness and transitions between NREM. This temporal and kinetic divergence further supports that our recorded signals isolate region-specific dopaminergic dynamics rather than generalized NE arousal activity.

Taken together, these physiological, functional, and kinetic distinctions indicate that while a negligible contribution from NE cannot be entirely ruled out, it is highly unlikely to account for a substantial portion of the DA2m signals observed during sleep-wake transitions in our study.

> *Similarly, the chemogenetic experiments rely on CNO to activate hM3Dq-expressing dopamine neurons. However, it is well established that CNO can be converted to clozapine in rodents, and clozapine itself is known to influence sleep/wake. Although the authors included non-hM3Dq-expressing mice as controls, the potential confounding effects of clozapine on sleep regulation remain a concern.*

We appreciate the reviewer raising this important point regarding the metabolism of CNO. We are aware of the evidence suggesting that CNO can undergo back-metabolism to clozapine in rodents, which could potentially exert independent effects on sleep-wake architecture. To mitigate this concern, we strictly employed several experimental safeguards:

(A) Non-hM3Dq Control Group: As noted by the reviewer, we included a cohort of mice that did not express the hM3Dq receptor but received the same dosage of CNO (1 mg/kg). In these animals, we observed no significant alterations in sleep-wake states compared to saline baseline (Figure S3), suggesting that at this dosage, any clozapine produced was below the threshold for behavioral modulation of sleep.

(B) Dosage Selection: We utilized a relatively low dose of CNO (1 mg/kg), which is widely reported in the literature to minimize the accumulation of clozapine to levels that would interfere with EEG-defined sleep states in rodents [5]. Furthermore, studies have demonstrated that while higher doses of CNO (e.g., 5–10 mg/kg) can produce clozapinelike effects on sleep architecture, lower doses around 1 mg/kg do not yield significant alterations in cortical EEG power distribution or sleep-wake amounts in control animals [6,7].

> *Midbrain dopamine neurons exhibit both tonic and phasic firing patterns. In Figure 1, most reported dopamine transitions appear relatively slow. However, some faster, phasic-like components are observable. For example, in NAc-L during REM-to-WAKE transitions, there are 2 phasic-like decreases between −20 and 0 s. The authors used*

> *laser-evoked stimulation experiments in the VTA and DRN and showed that 2 s versus 10 s stimulation produces distinct dopamine kinetics, suggesting that different firing patterns generate distinct DA dynamics. Moreover, the temporal profiles vary not only across regions but also across transitions within the same region. For example, in CeA, the NREM-to-WAKE transition shows a relatively rapid decrease, whereas REM-to-WAKE displays a much slower decline. Similarly, some regions (e.g., NAc-L NREM-to-WAKE, DRN REM-toWAKE) show faster changes, while others (e.g., mPFC WAKE-to-NREM, VTA NREM-toWAKE) show slower kinetics. These observations argue against a simple region-specific explanation and instead suggest that distinct firing modes may differentially contribute depending on transition type.*

We thank the reviewer for this insightful comment. We agree that midbrain dopamine neurons exhibit both tonic and phasic action-potential firing patterns. As summarized by Grace et al., dopamine neurons recorded using *in vivo* electrophysiology can display a slow, irregular, single-spike "tonic" firing pattern, typically around 2–10 Hz, as well as burst-like "phasic" firing patterns [8].

However, our recordings were performed using GRAB-DA2m fiber photometry. Therefore, our measurements reflect extracellular dopamine dynamics in the recorded target regions rather than the action-potential firing patterns of midbrain dopamine neurons. GRABDA2m has subsecond sensor kinetics and is suitable for detecting extracellular dopamine transients occurring over hundreds of milliseconds to seconds, as well as slower dynamics occurring over seconds to tens of seconds [1], which matches the timescale of the sleep–wake transition-related dynamics observed in previous studies [9,10]. Nevertheless, GRAB-DA2m fiber photometry in our study does not directly resolve dopamine neuron spike timing or distinguish tonic from phasic firing modes. Accordingly, we interpret our signals as extracellular dopamine concentration dynamics rather than as direct measurements of tonic or phasic neuronal firing.

Therefore, the transition-aligned dopamine signals shown in Figure 1 should be interpreted as dopamine dynamics occurring over seconds-to-tens-of-seconds around sleep–wake transitions, rather than as dopamine neuron firing patterns. In addition, these traces represent GRAB-DA2m signals averaged across sessions and mice within a ±30 s window centered on each sleep/wake transition. Thus, they do not necessarily represent individual dopamine transient patterns on single transitions. We also acknowledge the reviewer's observation that faster phasic-like components are visible in some traces, including the decreases in the NAc-L preceding REM-to-WAKE transitions. Direct electrophysiological recordings of dopamine neuron firing during sleep–wake transitions would be useful in future studies to determine how tonic and phasic firing modes contribute to the observed dopamine dynamics.

In the laser-evoked stimulation experiments shown in Figure 3, we thank the reviewer for the thoughtful interpretation. The results indicate that different stimulation durations can produce distinct dopamine release dynamics in downstream projection regions. Moreover, prolonged optogenetic stimulation was associated with more sustained dopamine responses, suggesting that the temporal profile of extracellular dopamine dynamics depends, at least in part, on the duration and region of dopaminergic input [1]. We also agree with the reviewer that the temporal profiles of the GRAB-DA2m signals vary not only across regions, but also across sleep/wake transitions within the same region. For example, in CeA, the NREM-to-WAKE transition shows a relatively rapid dopamine decrease, whereas the REM-to-WAKE transition displays a slower decline.

Similarly, faster dopamine changes are observed in some region/transition combinations, such as NAc-L during NREM-to-WAKE and DRN during REM-to-WAKE, whereas slower kinetics are observed in others, such as mPFC during WAKE-to-NREM and VTA during NREM-

to-WAKE. Together, these effects reflect both region-specific mechanisms and transition-dependent differences in dopaminergic activity.

> *While cross-correlation analysis provides insight into the temporal coordination of DA signals across regions, several limitations should be considered. Sleep/wake transitions are inherently non-stationary events, whereas cross-correlation assumes relatively stable signal properties within the analysis window. This mismatch may bias lag estimates and obscure transient lead-lag relationships. Moreover, the temporal resolution of fiber photometry and the kinetics of genetically encoded DA sensors limit the precision with which timing relationships can be interpreted, particularly for sub-second lags.*

We thank the reviewer for raising these important considerations. The temporal relationships between regional dopamine signals were assessed using cross-covariance analysis. We agree that cross-covariance analysis has limitations when applied to sleep/wake transitions, because these transitions are inherently non-stationary events. Although cross-covariance centers the signals by subtracting their means and is therefore less sensitive to baseline offsets than raw cross-correlation, it still summarizes the lagdependent covariance between two signals over the selected analysis window. Therefore, the inferred lag should be interpreted as a transition-level measure of temporal coordination rather than a precise estimate of instantaneous lead–lag timing.

To minimize the influence of brief or unstable state fluctuations, we only included transitions in which both the preceding and following sleep/wake epochs lasted at least 30 s, and excluded epochs shorter than 30 s [4]. This criterion helped ensure that the analyzed events represented well-defined transitions between sustained behavioral states rather than transient or fragmented episodes. Although dopamine signals may still change dynamically within the transition window, and the temporal resolution of fiber photometry and the kinetics of genetically encoded GRAB-DA2m sensors limit the precision with which fine-scale timing relationships can be interpreted, dopamine signals were relatively stable within each behavioral state, as shown in Fig. 1B and reported previously [1,9,10] Thus, we believe that cross-covariance analysis provides useful information about the temporal coordination of dopamine dynamics across regions.

> *In the Introduction, the authors state that they aim to address 'which dopaminergic populations causally drive these patterns.' However, the chemogenetic approach used operates on a relatively slow timescale: CNO-induced activation takes 15-30 minutes to produce effects, and the induced changes are long-lasting. In contrast, the dopamine transitions described in Figure 1 occur on a much faster timescale compared to CNO manipulation. Thus, while chemogenetic activation demonstrates that stimulating VTA or DRN dopamine neurons promotes wakefulness, it does not directly establish that these populations causally drive the rapid transition-related DA dynamics observed in the photometry recordings.*

We thank the reviewer for this thoughtful comment. We agree that chemogenetic manipulation operates on a much slower timescale than the rapid dopamine transients observed during sleep–wake transitions, and therefore does not directly recapitulate these fast dynamics. In particular, CNO-induced activation unfolds over minutes and produces sustained changes in neuronal activity, whereas the DA signals we report fluctuate on a sub-second to second timescale. Our intention with the chemogenetic experiments was not to mimic the precise temporal profile of endogenous DA signals, but rather to test whether increasing the activity of specific dopaminergic populations is sufficient to influence behavioral state.

In this context, our results show that activation of VTA or DRN dopaminergic neurons robustly promotes wakefulness, supporting a causal role for these populations in sleep– wake regulation at the circuit level. However, we agree that these data do not by themselves

establish that these neurons directly generate the rapid transition-related DA dynamics observed in the photometry recordings.

> ***Reviewer #2 (Public review):***
>
> *In "Brainwide dopamine dynamics across sleep-wake transitions", Chen et al. provide a thorough description of how dopamine dynamics fluctuate across sleep-wake transitions and in transitions between sleep states. To achieve this, the authors used multi-channel fiber photometry and a genetically encoded fluorescent dopamine reporter to simultaneously measure dopamine dynamics in 8 brain regions. They also used EEG measurements to precisely quantify and time transitions between sleep states and wakefulness. Finally, the authors used channelrhodopsin to examine dopamine dynamics following subregion stimulation and chemogenetics to test the causal relationship between activation of distinct dopamine neuron populations and their effects on sleep state.*
>
> *The conclusions made by the authors in this study are modest and appropriate given the largely observational nature of the principal findings. The use of optogenetics to probe regional dopamine signaling following activation of distinct nuclei is interesting, but not entirely novel and constrained in interpretability. Similarly, the chemogenetics experiment largely confirms previous studies, which the authors correctly cited in the text.*
>
> *The principal findings of this study are based on strong methodological and analytical methods. Implanting 8 optical fibers in a single mouse, along with EEG/EMG electrodes, is technically challenging, providing valuable, simultaneous measurements of dopamine fluctuations across the brain. This enables the strong correlational and time-locked analyses performed by the authors in Figure 2. What's more, the use of EEG/EMG electrodes provides time-locked descriptions of sleep states, enabling precise comparisons between the dopamine signal and sleep state transitions.*
>
> *The paper has some weaknesses that the authors could address. The analyses in Figure 1 could be strengthened to show how dopamine changes during transitions between specific sleep states. The injection sites for channelrhodopsin and chemogenetic viruses could be validated to strengthen the interpretation of those results. Also, a stronger justification for the experiments conducted in Figure 3 could be provided, as they seem unrelated to the present study.*
>
> *Overall, this study has strong descriptive power, convincingly showing how dopamine fluctuates across sleep states. Some of the other aspects of the paper, however, are somewhat limited in novelty and interpretation.*
>
> *The analyses in Figure 1 could be strengthened to show how dopamine changes during transitions between specific sleep states.*

We appreciate the reviewer's thoughtful suggestion. We agree that the directionality and kinetics of dopamine changes during sleep/wake transitions may provide important information beyond state-level dopamine quantification.

In this study, mice were recorded for 4–5 h during each sleep session. Across the recording period, mice frequently transitioned from NREM to WAKE, WAKE to NREM, NREM to REM, and REM to WAKE. Transitions from WAKE to REM were rarely observed and therefore were not included in the transition analysis. Accordingly, we focused our analysis on the four major transition types: NREM-to-WAKE, WAKE-to-NREM, NREM-toREM, and REM-to-WAKE [4,9,11].

For each transition type, dopamine dynamics were analyzed separately by aligning the zscored GRAB-DA2m signal to the transition onset and averaging across all epochs of the same transition type. To minimize the influence of brief or unstable state fluctuations, we excluded transitions in which either the preceding or following sleep/wake epoch lasted less than 30 s. The resulting transition-triggered dopamine traces were then averaged across sessions and mice for each transition type independently.

Thus, the transition analysis preserves the directionality of state changes rather than pooling all sleep/wake transitions together. Because dopamine signals differ across behavioral states, transitions between neighboring states produce distinct temporal profiles when aligned to the transition point [4,9-11]. For example, REM-to-WAKE transitions may show a rapid increase in dopamine in the mPFC, whereas WAKE-to-NREM or NREM-to-REM transitions may show slower and more modest decreases. These transition - specific kinetics may reflect distinct underlying mechanisms, including changes in dopamine neuron firing or local terminal modulation.

> *The injection sites for channelrhodopsin and chemogenetic viruses could be validated to strengthen the interpretation of those results.*

We agree with the reviewer that precise histological validation is essential for the correct interpretation of our optogenetic and chemogenetic findings.

Regarding the chemogenetic experiments, as noted, we provide examples of virus expression in the VTA, DRN, and SNc in Figure 4. By demonstrating the consistency and restriction of our targeting across the entire cohort (VTA, SNc, and DRN), we confirmed that our observed sleep effects were regionally specific. Our data only included mice with accurate targeting and no substantial virus "leakage" into adjacent nuclei.

We thank the reviewer for this insightful observation regarding the regional dopamine (DA) responses following SNc stimulation. While the SNc is traditionally associated with the dorsal striatum (DLS), several studies have demonstrated that SNc dopaminergic neurons also project to the nucleus accumbens, particularly the lateral shell [12,13]. Furthermore, recent work characterizing the functional heterogeneity of midbrain DA neurons suggests that SNc subpopulations can drive significant DA release in ventral striatal subregions [14]. We appreciate the reviewer's caution regarding potential off-target effects. While our histological criteria for validation post recordings were stringent, we acknowledge that in any midbrain manipulation, the close anatomical proximity of the VTA and SNc makes it technically challenging to guarantee zero involvement of neighboring VTA neurons. However, by using mice with the most restricted virus expression and fibers targeting, we have minimized this potential confound as much as is technically feasible with current viral and optogenetic methods.

> *Also, a stronger justification for the experiments conducted in Figure 3 could be provided, as they seem unrelated to the present study.*

We thank the reviewer for this comment. The experiments in Figure 3 were designed to systematically map the sources of dopaminergic inputs to key brain regions examined in this study [15], including the mPFC, DLS, NAc, and CeA. Establishing these input–output relationships is important for interpreting the photometry signals observed during sleep–wake transitions.

Specifically, we found that optogenetic activation of VTA dopaminergic neurons elicits DA responses in all four regions, whereas activation of DRN dopaminergic neurons induces responses in the mPFC, DLS, and CeA, and activation of SNc dopaminergic neurons induces responses in the mPFC, NAc, and DLS. These results reveal partially overlapping but distinct projection patterns across dopaminergic populations.

Taken together, these data provide a circuit-level framework suggesting that VTA, SNc, and DRN dopaminergic neurons may contribute differentially and with distinct weights to the DA signals observed in these regions during sleep wake transitions.

> *Overall, this study has strong descriptive power, convincingly showing how dopamine fluctuates across sleep states. Some of the other aspects of the paper, however, are somewhat limited in novelty and interpretation.*

We appreciate the reviewer's assessment that our study convincingly demonstrates how dopamine fluctuates across sleep states. We agree that the primary contribution of this work is descriptive and foundational. At the same time, we respectfully emphasize that rigorous, comprehensive descriptive studies are essential, particularly when addressing phenomena that have not been systematically characterized. Prior to this work, dopamine dynamics during natural sleep–wake transitions had not been measured simultaneously across multiple brain regions.

Our multi-site photometry approach advances the field in several important ways. Technically, the combination of simultaneous eight-region fiber photometry with EEG/EMG recordings represents a substantial methodological advance, enabling brainwide, network-level analysis of dopamine dynamics during natural state transitions. This approach reveals emergent features—such as temporal coordination and inter-regional lead–lag relationships—that cannot be captured using single-site recordings. Moreover, integrating brain-wide measurements with region-specific manipulations allows circuitlevel insights that would not be accessible from either approach alone.

Conceptually, our findings revealed the region, sleep/wake transition type -specific and bidirectional dopamine dynamics, instead of the prevailing view of dopamine as a uniform arousal signal: dopamine decreases in certain limbic regions, such as the central amygdala and nucleus accumbens lateral shell, during arousal transitions, while increasing in cortical and other striatal regions. These results refine simplified models of dopaminergic regulation of arousal. In addition, our data reveal differential circuit contributions, with the VTA and DRN—but not the SNc—promoting wakefulness, highlighting functional specialization within the dopamine system.

We acknowledge that some aspects of our study, including the optogenetic mapping and chemogenetic experiments, build on established methodologies and in part confirm prior findings. However, these experiments also provide several new insights. First, whereas individual dopamine sources have often been studied in isolation, our systematic comparison across VTA, SNc, and DRN using consistent methods reveals distinct brainwide functional contributions that were not previously established. Second, our optogenetic mapping does not simply recapitulate known projection patterns, but instead uncovers quantitative differences in dopamine release kinetics and magnitude across source–target pairs, which inform the heterogeneity of the transition dynamics. Finally, our findings provide a crucial anatomical and temporal framework for future research on the specific mechanisms driving these dynamics and their precise functional consequences.

References:

(1) Sun, F. et al. Next-generation GRAB sensors for monitoring dopaminergic activity in vivo. Nat Methods 17, 1156-1166, doi:10.1038/s41592-020-00981-9 (2020).

(2) Ihalainen, J. A., Riekkinen, P., Jr. & Feenstra, M. G. Comparison of dopamine and noradrenaline release in mouse prefrontal cortex, striatum and hippocampus using microdialysis. Neurosci Lett 277, 71-74, doi:10.1016/s0304-3940(99)00840-x (1999).

(3) Berridge, C. W. & Abercrombie, E. D. Relationship between locus coeruleus discharge rates and rates of norepinephrine release within neocortex as assessed by in vivo microdialysis. Neuroscience 93, 1263-1270, doi:10.1016/s0306-4522(99)00276-6 (1999).

(4) Silverman, D. et al. Activation of locus coeruleus noradrenergic neurons rapidly drives homeostatic sleep pressure. Sci Adv 11, eadq0651, doi:10.1126/sciadv.adq0651 (2025).

(5) Anaclet, C. et al. The GABAergic parafacial zone is a medullary slow wave sleeppromoting center (vol 17, pg 1217, 2014). Nat Neurosci 17, 1841-1841, doi:DOI 10.1038/nn1214-1841d (2014).

(6) Ma, C. Y. et al. Microglia regulate sleep through calcium-dependent modulation of norepinephrine transmission. Nat Neurosci 27, 249-258, doi:10.1038/s41593-02301548-5 (2024).

(7) Traut, J. et al. Effects of clozapine-N-oxide and compound 21 on sleep in laboratory mice. Elife 12, doi:10.7554/eLife.84740 (2023).

(8) Grace, A. A., Floresco, S. B., Goto, Y. & Lodge, D. J. Regulation of firing of dopaminergic neurons and control of goal-directed behaviors. Trends Neurosci 30, 220-227, doi:10.1016/j.tins.2007.03.003 (2007).

(9) Darmohray, D. et al. Brainstem circuit for sickness-induced sleep. Sci Adv 11, doi:ARTN eady024510.1126/sciadv.ady0245 (2025).

(10) Hasegawa, E. et al. Rapid eye movement sleep is initiated by basolateral amygdala dopamine signaling in mice. Science 375, 994-+, doi:10.1126/science.abl6618 (2022).

(11) Ding, X. et al. Neuroendocrine circuit for sleep-dependent growth hormone release. Cell 188, 4968-4979 e4912, doi:10.1016/j.cell.2025.05.039 (2025).

(12) Poulin, J. F. et al. Mapping projections of molecularly defined dopamine neuron subtypes using intersectional genetic approaches. Nat Neurosci 21, 1260-1271, doi:10.1038/s41593-018-0203-4 (2018).

(13) Lerner, T. N. et al. Intact-Brain Analyses Reveal Distinct Information Carried by SNc Dopamine Subcircuits. Cell 162, 635-647, doi:10.1016/j.cell.2015.07.014 (2015).

(14) Azcorra, M. et al. Unique functional responses differentially map onto genetic subtypes of dopamine neurons. Nat Neurosci 26, 1762-1774, doi:10.1038/s41593023-01401-9 (2023).

(15) Eban-Rothschild, A., Rothschild, G., Giardino, W. J., Jones, J. R. & de Lecea, L. VTA dopaminergic neurons regulate ethologically relevant sleep-wake behaviors. Nat Neurosci 19, 1356-1366, doi:10.1038/nn.4377 (2016).

https://doi.org/10.7554/eLife.110675.1.sa0